Study of low-energy antineutrino interactions on protons

G. Fanourakis* and L. K. Resvanis

Physics Laboratory, University of Athens, Athens 144, Greece

G. Grammatikakis,[†] P. Tsilimigras, and A. Vayaki

Nuclear Research Center Democritos, Aghia Paraskevi Attikis, Athens, Greece

U. Camerini, W. F. Fry, R. J. Loveless, J. H. Mapp,[‡] and D. D. Reeder

Department of Physics, University of Wisconsin, Madison, Wisconsin 53706

(Received 3 July 1979; revised manuscript received 31 October 1979)

We present a study of antineutrino interactions in hydrogen obtained in a 138 000-picture run at the BNL 7-ft bubble chamber. The antineutrino beam had an energy distribution that peaked at ~ 1.1 GeV. The cross section measured for charged-current interactions is $\sigma(\bar{\nu}p \to \mu^+ + \text{anything}) = (0.32 \pm 0.08) \times 10^{-38} \times [E_{\bar{\nu}} \text{ (GeV)}]$ cm^2. The neutral-current cross section is $\sigma(\bar{\nu}p \to \bar{\nu}p\pi^+\pi^-) = 5.5^{+4.4}_{-2.6} \times 10^{-40}$ cm^2. The ratio of strangeness-changing to non-strangeness-changing charged currents is $R_s = 0.06^{+0.13}_{-0.05}$. An upper limit determined for charm production is $\sigma_c < 3.8 \times 10^{-40}$ cm^2 at the 90% confidence level. From the momentum-transfer distribution we measure average Q^2 for inelastic charged-current events with energy greater than 2 GeV, $\langle Q^2 \rangle = (0.10 \pm 0.03)[E_{\bar{\nu}} \text{ (GeV)}] + (0.10 \pm 0.09)$ (GeV/c)^2. Using a maximum-likelihood method we determine from the quasielastic events $\bar{\nu}p \to \mu^+ n$ an axial-vector mass $M_A = 0.9^{+0.4}_{-0.3}$ GeV/c^2.

I. INTRODUCTION

We have studied the interactions of antineutrinos on protons at low energy (~1.3 GeV) in a hydrogen bubble chamber. This is the only low-energy antineutrino experiment in hydrogen, although other experiments[1-7] have studied low-energy antineutrinos interacting in nuclei. Extensive studies of low-energy neutrino interactions have been reported.[7-12]

In general, antineutrino reactions are more difficult to study than neutrino reactions because the antineutrino flux is lower (~40%) than the neutrino flux and the cross section is smaller (~30%). Hence the number of $\bar{\nu}$ interactions per picture or per second is approximately 0.1 that for ν. For hydrogen an additional difficulty arises from charge and lepton-number conservation. Because of the μ^+ in the final state all antineutrino reactions (except neutral currents) have a zero hadronic charge. This means that a substantial fraction of the cross section occurs in final states with only neutral hadrons (i.e., $\bar{\nu}p \to \mu^+ n\pi^0$), which are unobservable in the bubble chamber. In contrast, for neutrino reactions the final-state μ^- results in a hadronic charge of +2 so comparable interactions have at least two charged hadronic tracks and are thus observable in the bubble chamber.

The major topics presented in this experiment are (1) inelastic charged-current reactions, which have a μ^+ in the final state, (2) inelastic neutral-current reactions, of which only $\bar{\nu}p \to \bar{\nu}p\pi^+\pi^-$ is presented, (3) flavor-changing interactions, which have observable strange particles, and (4) quasi-

elastic reactions ($\bar{\nu}p \to \mu^+ n$), which have visually only a single identified μ^+. The determination of the flux of antineutrinos allows us to compute absolute cross sections for each of these processes.

The cross section for the quasielastic reaction can be computed as a function of a single parameter, an effective axial-vector mass M_A. The experimental result for M_A is compared to theoretical predictions and to results from neutrino experiments on equivalent reactions ($\nu n \to \mu^- p$).

II. EXPERIMENTAL APPARATUS

The antineutrinos were produced by the BNL broad-band, horn-focused beam from the 30-GeV/c proton beam at the AGS. The average antineutrino energy was 1.3 GeV. The antineutrinos were directed into the BNL 7-ft hydrogen bubble chamber where 138 000 pictures were exposed.

The determination of the antineutrino flux and energy is crucial for the calculation of an absolute cross section. The first step was the measurement of the neutrino spectrum in a previous experiment.[13] This experiment utilized the quasielastic reaction $\nu n \to \mu^- p$ observed in the same bubble chamber filled with deuterium. From a theoretical model the cross section for quasielastic events was calculated. The observed number of such reactions can then be directly related to the neutrino flux.

From Cabibbo theory[14] and the isotriplet hypothesis, the quasielastic cross section can be computed with only the q^2 dependence of the weak axial-vector form factor not fixed. (See Sec. VII.)

The standard parametrization of the q^2 dependence as a dipole form factor with an axial mass $M_A = 1.08$ was used[12]:

$$g_1(q^2) = \frac{g_1(0)}{1 - q^2/M_A^2} .$$

By integrating this cross section, weighted by the observed reactions, over energy they calculate the neutrino flux determined to be

$$\Phi = \int \frac{N(E)}{\sigma(E)}$$

$$\times \, dE /(\text{No. of target nucleons}) (\text{No. of pulses}).$$

They obtained 8.3×10^5 ν/cm^2 pulse for 8×10^{12} protons incident on the target in their experiment.

We now calculate the antineutrino spectrum by scaling this experimentally deduced neutrino spectrum with the ratio of antineutrino to neutrino spectrum as obtained from a Monte Carlo.[13] This ratio is not sensitive to the spectral shape introduced into the Monte Carlo. We find that the antineutrino flux, integrated over energy, is 2.4×10^5 antineutrinos/cm^2 pulse for 5×10^{12} protons on target per pulse (5×10^{12} protons/pulse is a typical proton flux in our experiment); the antineutrino flux-energy (product of antineutrino flux and antineutrino energy) is 3.4×10^5 antineutrinos GeV/cm^2 pulse. The errors in these calculations are estimated to be ~12%. These errors include uncertainties due to assumptions in the Monte Carlo program and statistical errors in the experimentally determined neutrino flux. We estimate that approximately 10% of the charged-current interactions in this experiment come from neutrino contamination.

Four steel plates, each 2 in. thick, were installed at the downstream end of the chamber to identify the muons (approximately one absorption length). The plates were separated by ~4 in. to allow visual observation of tracks between each plate. Owing to the limited solid angle subtended by the plates, approximately $\frac{1}{2}$ of the muons produced in antineutrino interactions intersected all of the plates. The effective fiducial volume of the chamber was 5 m³ (0.29 metric tons) and the magnetic field at the center of the chamber was 27 kG.

III. DATA ANALYSIS

A double scan was made for interactions with two or more prongs which were not obviously elastic scatters from incoming charged tracks. 160 such events were found with a double scan efficiency of $0.97^{+0.03}_{-0.05}$. All events were measured on film-plane digitizers, reconstructed by the TVGP geometry program, and processed through the kinematic fitting program SQUAW . Assuming the
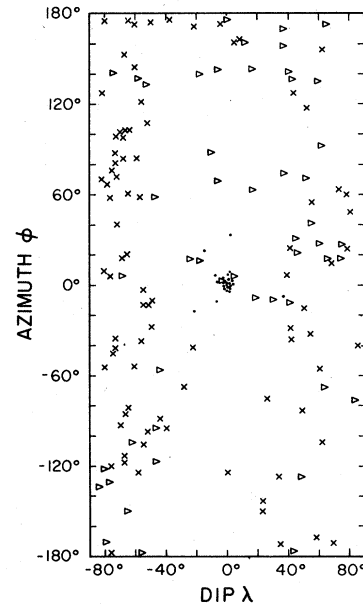

FIG. 1. Dip λ and azimuth ϕ plotted for the 160 inelastic events. Dots denote the 24 fitted events and triangles indicate coplanar events with $-0.1 < \cos\beta < +0.1$.

hypothesis that the event was initiated by a neutral particle incident along the expected antineutrino direction, 24 events remain which fit [either three-constraint (3C) or 0C].

To illustrate the effectiveness of the selection procedure let us first consider the cosmic-ray background. Most of the cosmic-ray background produces events whose incoming track, charged or neutral, appears to enter the chamber at a large angle with respect to the antineutrino beam. To identify this background we computed the azimuth ϕ and the dip λ of the total visible momentum of each event. In Fig. 1 we display the distribution in ϕ and λ for the 160 measured events, distinguishing those events which have a fit in SQUAW from those which do not. True antineutrino interactions are expected to cluster around $\phi = 0°$, $\lambda = 0°$.

As another demonstration of the efficacy of the fitting procedure consider incoming charged particles, primarily from cosmic rays, which interact and produce an event which appears as a three-prong topology. This hadronic background is most-
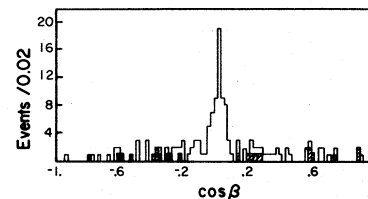

FIG. 2. Coplanarity distribution for the events. The shaded regions show the fitted events.

TABLE I. List of 24 multiprong candidates.

	Fit class	Number of events
Charged-current events		
$\nu p \to \mu^-$ anything	3C, 0C	2
$\bar{\nu} p \to \mu^+ \Lambda$ $\hookrightarrow p\pi^-$	6C	1
$\bar{\nu} p \to \mu^+ p \pi^-$	3C	10
$\bar{\nu} p \to \mu^+ p \pi^- \pi^0$	0C	2 [a]
$\bar{\nu} p \to \mu^+ n \pi^+ \pi^-$	0C	3
Neutral-current events		
$\bar{\nu} p \to \bar{\nu} p \pi^+ \pi^-$	0C	4
Background events		
$np \to pp\pi^-$	3C	2

[a] The π^0 is identified by a Dalitz pair in one event.

ly coplanar because the interactions are largely elastic. This coplanarity can be exhibited by defining

$$\cos\beta = \frac{\vec{p}_1 \cdot \vec{p}_2 \times \vec{p}_3}{|\vec{p}_1||\vec{p}_2 \times \vec{p}_3|},$$

where $\vec{p}_1, \vec{p}_2, \vec{p}_3$ are the momenta of the three charged tracks. Figure 2 shows a plot of $\cos\beta$ for the 160 events, again distinguishing fitted and nonfitted events. True antineutrino events are not expected to have $\cos\beta$ near zero.

The results for the 24 fitted candidates are tabulated in Table I. The only antineutrino interactions which are not correctly identified by this procedure have two or more missing neutrals, an unlikely occurrence because of phase-space suppression. There is no evidence for such events and we estimate less than one event of this type in this experiment. As a check we note that antineutrino events ($\bar{\nu} p \to \mu^+ p \pi^- \pi^0 \pi^0$) with two missing neutrals are as likely as events with five outgoing charged tracks ($\bar{\nu} p \to \mu^+ p \pi^- \pi^+ \pi^-$); no such five-prong events are observed.

A separate scan for single tracks penetrating the plates was done for the complete sample to identify quasielastic candidates ($\bar{\nu} p \to \mu^+ n$). Approximately half the film was double-scanned; the estimated overall scanning efficiency was 0.90 ± 0.10. A total of 23 single track events were found with a vertex inside a reduced fiducial volume of 3.75 m^3. These events were measured and processed through SQUAW kinematics and 22 events have a 0C fit to $\bar{\nu} p \to \mu^+ n$. However, to eliminate cosmic-ray background we required candidates to have $|\phi| < 45°$ and $|\lambda| < 45°$ (see Fig. 1). Four events have $\lambda < -45°$, which is expected for cosmic-ray tracks, and one has a large azimuth. Seventeen

candidates for $\bar{\nu} p \to \mu^+ n$ remain.

IV. INELASTIC CHARGED CURRENTS

Sixteen candidates were fitted as antineutrino charged-current interactions. Eight (50%) of these have an identified muon, i.e., a track which traverses all four iron plates. One candidate has a fitted $\Lambda^0 \to p\pi^-$ decay giving a $\chi^2 = 9.6$ for six constraints. Two candidates fit as neutrino interactions; one a 3C fit ($\nu p \to \mu^- p \pi^+$), the other a 0C ($\nu p \to \mu^- p \pi^+ \pi^0$) with one identified γ conversion in the hydrogen. These two events are consistent with the expected 10% neutrino background.

Fifteen antineutrino non-strangeness-changing charged-current interactions remain. The energy spectrum of these events is shown in Fig. 3. In order to determine the inelastic charged-current cross section, corrections must be made for the unobserved final states, $\bar{\nu} p \to \mu^+ n \pi^0$ and $\bar{\nu} p \to \mu^+ n \pi^0 \pi^0$.

The ratio $R^+ = \sigma(\bar{\nu} p \to \mu^+ p \pi^-)/(\bar{\nu} p \to \mu^+ n \pi^0)$ is determined by the isospin properties of the charged weak current. Adler's prediction[15] for this ratio varies from 0.81 to 0.94 depending on different methods of modifying the Born approximation to
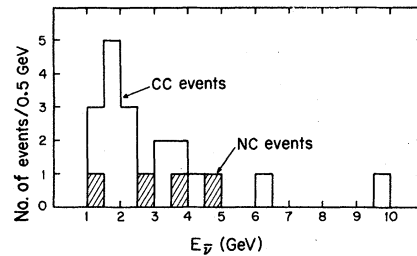

FIG. 3. Energy spectra of charged-current and neutral-current events (shaded areas).

conform to the soft-pion limit. A recent 12-ft bubble chamber experiment[11] on neutrino interactions measures $R^+ = 0.89 \pm 0.17$. Using $R^+ = 0.89$ we estimate 11 ± 3 $\bar{\nu}p \to \mu^+ n\pi^0$ events for this experiment. At low energies the reaction $\bar{\nu}p \to \mu^+ n\pi^0\pi^0$ is limited by phase space, and we estimate less than one event for this experiment.

For 27 ± 7 events the inelastic charged-current cross section becomes

$$\sigma(\bar{\nu}p \to \mu^+ + \text{anything}) = (0.45 \pm 0.12) \times 10^{-38} \text{ cm}^2$$

at an average $\bar{\nu}$ energy of 1.3 GeV. A parametrization which explicitly displays the energy dependence of the cross section is:

$$\sigma_{\bar{\nu}p} = (0.32 \pm 0.08) \times 10^{-38} [E_{\bar{\nu}} \text{ (GeV)}] \text{ cm}^2.$$

This agrees with CERN-Gargamelle[5] results

$$\sigma_{\bar{\nu}p} = (0.26 \pm 0.02) \times 10^{-38} [E_{\bar{\nu}} \text{ (GeV)}] \text{ cm}^2,$$

obtained at energies to 8 GeV and with IHEP-Serpukhov and ITEP-Moscow collaboration[6] results

$$\sigma_{\bar{\nu}p} = (0.31 \pm 0.03) \times 10^{-38} [E_{\bar{\nu}} \text{ (GeV)}] \text{ cm}^2,$$

obtained in a counter experiment at energies to 30 GeV.

A plot of $\langle Q^2 \rangle$, the mean square of momentum transfer, as a function of antineutrino energy for $\bar{\nu}p \to \mu^+ p\pi^-$ is shown in Fig. 4. A linear fit above 2 GeV gives $\langle Q^2 \rangle = (0.10 \pm 0.03)[E_{\bar{\nu}} \text{ (GeV)}] + (0.10 \pm 0.09) \text{ (GeV/}c)^2$. This is to be compared with the Gargamelle result $\langle Q^2 \rangle = (0.15 \pm 0.04)[E_{\bar{\nu}} \text{ (GeV)}] + (0.05 \pm 0.12) \text{ (GeV/}c)^2$.[5]

V. NEUTRAL CURRENTS

Four interactions fit the neutral-current hypothesis $\bar{\nu}p \to \bar{\nu}p\pi^+\pi^-$ (see Table I). Three of the π^+ decay visibly ($\pi\mu e$), and the fourth interacts in the first plate. All protons stop in the chamber. The antineutrino energy spectrum for these events is shown in Fig. 3 and is consistent with the energy spectrum for the charged-current events.

The major background consists of incident neutrons producing an inelastic interaction. From the entire sample two such interactions fit $np \to pp\pi^-$
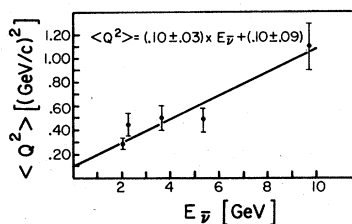

FIG. 4. $\langle Q^2 \rangle$ vs $E_{\bar{\nu}}$ for $E_{\bar{\nu}} > 2$ GeV and a linear fit giving $\langle Q^2 \rangle = (0.10 \pm 0.03) [E_{\bar{\nu}} \text{ (GeV)}] + (0.10 \pm 0.09) \text{ (GeV/}c)^2$.

(see Table I) with neutron energies of 1.3 and 1.8 GeV/c. The only neutron-induced topology which simulates the three-prong neutral-current interaction is $np \to np\pi^+\pi^-$. Because of the low neutron energy and the phase-space limitation relative to $np \to pp\pi^-$, we estimate less than 0.7 background events due to $np \to np\pi^+\pi^-$ and $np \to np\pi^+\pi^-\pi^0$.

Other possible neutral-current interactions ($\bar{\nu}p \to \bar{\nu}p$, $\bar{\nu}p \to \bar{\nu}p\pi^0$, $\bar{\nu}p \to \bar{\nu}n\pi^+$, $\bar{\nu}p \to \bar{\nu}n\pi^+\pi^0$, etc.) require the observation of only a single hadronic track in the bubble chamber. Backgrounds from neutron-induced interactions are substantial, and identification of these neutral-current reactions is not possible in this experiment.

Hence we give a partial cross section for the neutral-current reaction:

$$(\bar{\nu}p \to \bar{\nu}p\pi^+\pi^-) = (5.5^{+4.4}_{-2.6}) \times 10^{-40} \text{ cm}^2.$$

VI. FLAVOR-CHANGING REACTIONS

Since the weak interactions can change flavors (strangeness, charm) we expect production of single particles exhibiting these new flavors. Although charm production is expected to be small (and hence unobservable with the statistics in this experiment) at the relatively low energy of this experiment, strangeness production should be observable although small due to the suppression by the sine of the Cabibbo angle.

Because of the phase-space limitation, the two-body final state, $\bar{\nu}p \to \mu^+\Lambda$, should be more probable than three- or four-body final states ($\bar{\nu}p \to \mu^+ pK^-$, $\bar{\nu}p \to \mu^+ p\pi^- \bar{K}^0$, $\bar{\nu}p \to \mu^+\Sigma^-\pi^+$, etc.). Many of these final states have a neutral strange decay which would be clearly visible downstream of the vertex. The charged strange particles can be identified by a kinematic fit in SQUAW (K^-) or by subsequent decays (Σ^+, Σ^-).

One event was found in the scan which gave a 6C fit to $\bar{\nu}p \to \mu^+\Lambda^0$, $\Lambda^0 \to p\pi^-$. The μ^+ traversed all four iron plates. The antineutrino energy was determined to be 3.34 ± 0.03 GeV. This event satisfies $\Delta Q = \Delta S$ as expected for strangeness-changing reactions. We estimate the cross section for this interaction to be

$$\sigma(\bar{\nu}p \to \mu^+\Lambda^0) = (2.6^{+5.9}_{-2.1}) \times 10^{-40} \text{ cm}^2.$$

The Gargamelle result[3] in a heavy-liquid bubble chamber is $\sigma = (2.07 \pm 0.76) \times 10^{-40} \text{ cm}^2$. Since no other strangeness-changing reactions were observed, we present this cross section as the best estimate for the strangeness-changing cross section for this experiment. Thus the ratio, for charged-current reactions, of strange to nonstrange particle production is

$$R_s = 0.06^{+0.13}_{-0.05}.$$

Charm-particle production in antineutrino inter-actions is expected to occur only from $s\bar{s}$ ocean quarks, which implies a rate of approximately 1–2% of charged-current reactions. The most obvious charm signature for this experiment is the observation of events with $\Delta Q = -\Delta S$. Other signatures, such as invariant-mass peaks, dilepton events, or visible decay lengths, require sub-stantially more data or additional experimental apparatus.

No events with any charm signature were ob-served so the upper limit for antineutrino charm production at 90% confidence level is

$$\sigma(\bar{\nu}p \rightarrow \mu^+ + \text{charm}) < 3.8 \times 10^{-40} \text{ cm}^2$$

at antineutrino energies of approximately 1.3 GeV. This limit is 8% of the charged-current rate. A recent BNL neutrino experiment[9,10] at a compar-able energy finds evidence for charm production with a rate of 3.5% of the charged-current rate.

VII. QUASIELASTIC REACTION ($\bar{\nu}p \rightarrow \mu^+ n$)

In the $V - A$ theory each transition is character-ized by six form factors

$$\langle n | V_\mu | p \rangle \sim \gamma_\mu f_1(q^2) + i \frac{\sigma_{\mu\nu} q^\nu}{M_p + M_n} f_2(q^2)$$

$$+ \frac{q_\mu}{M_p + M_n} f_3(q^2),$$

$$\langle n | A_\mu | p \rangle \sim \gamma_\mu \gamma_5 g_1(q^2) + i \frac{\sigma_{\mu\nu} q^\nu \gamma_5}{M_p + M_n} g_2(q^2)$$

$$+ \frac{q_\mu \gamma_5}{M_p + M_n} g_3(q^2), \qquad (1)$$

where M_p and M_n are masses of proton and neu-tron, and q_μ is the momentum transfer from p to n. We assume second-class currents do not exist ($g_2 = 0, f_3 = 0$) and the pseudoscalar form factor is negligible ($g_3 = 0$). Cabibbo theory[14] specifies the form factors

$$f_1(q^2) = \cos\theta_C \left[F_1^p(q^2) - F_1^n(q^2) \right],$$

$$f_2(q^2) = \cos\theta_C \left[F_2^p(q^2) - F_2^n(q^2) \right], \qquad (2)$$

$$g_1(0) = \cos\theta_C (F + D),$$

where $F_i^{p,n}(q^2)$ are electromagnetic form factors, θ_C is the Cabibbo angle, and $F + D = 1.26$. Accord-

FIG. 5. Q^2 distribution for quasielastic events ($\bar{\nu}p \rightarrow \mu^+ n$). A theoretical cross section $d\sigma/dQ^2$ is shown for three values of M_A. The theoretical cross section is corrected according to the detection efficiency of the experimental apparatus.

ing to the conserved-vector-current hypothesis the weak vector form factors can be written:

$$G_E^i(q^2) = F_1^i(q^2) + \frac{q^2}{4M^2} F_2^i(q^2),$$

$$G_M^i(q^2) = F_1^i(q^2) + F_2^i(q^2),$$

where $i = p, n$. For low energies $G_{E,M}^i(q^2)$ can be described by a dipole fit,

$$G_E^p = D, \quad G_M^p = (1 + \mu_p)D,$$

$$G_E^n = 0, \quad G_M^n = \mu_n D,$$

where $D = (1 - q^2/M_V^2)^{-2}$, μ_p and μ_n are the ano-malous magnetic moments, and $M_V = 0.84$ GeV/c^2. We introduce, as usual, a dipole q^2 dependence for the weak axial-vector form factor

$$g_1(q^2) = \frac{g_1(0)}{(1 - q^2/M_A)^2}.$$

M_A is the only unspecified parameter in the matrix element. From the q^2 dependence of the data we will determine M_A.

We now write down the cross section for the quasielastic reaction

$$\frac{d\sigma}{dQ^2} = \frac{G^2 M^2}{8\pi E^2} \left[A(Q^2) - B(Q^2) \left(\frac{s-u}{M^2} \right) \right.$$

$$\left. + C(Q^2) \left(\frac{s-u}{M^2} \right)^2 \right], \qquad (3)$$

where

$$A(Q^2) = \frac{Q^2 + m_\mu^2}{4M^2} \left[f_1^2 \left(-4 + \frac{Q^2}{M^2} \right) + f_1 f_2 \left(\frac{4Q^2}{M^2} \right) + f_2^2 \frac{Q^2}{M^2} \left(1 - \frac{Q^2}{4M^2} \right) + g_1^2 \left(4 + \frac{Q^2}{M^2} \right) - \frac{m_\mu^2}{M^2} [(f_1 + f_2)^2 + g_1^2] \right],$$

$$B(Q^2) = (f_1 + f_2) g_1 \frac{Q^2}{M^2},$$

$$C(Q^2) = \frac{1}{4} \left[f_1^2 + f_2^2 \frac{Q^2}{4M^2} + g_1^2 \right],$$
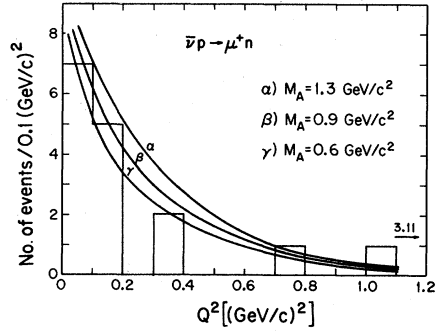
with $Q^2 = -q^2$, M = nucleon mass, m_μ = muon mass.

The experimental Q^2 distribution for the 17 can-didates is shown in Fig. 5. Because of the experi-mental detection efficiency for muons and the pres-ence of background interactions ($\bar{\nu}p \rightarrow \mu^+ n\pi^0$), the
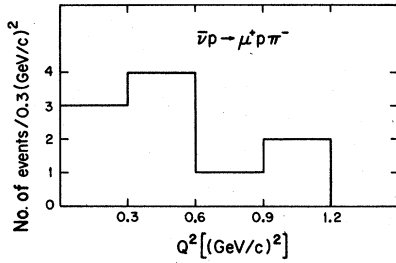
FIG. 6. Q^2 distribution of the observed $\bar{\nu}p \to \mu^+ p\pi^-$ events.

FIG. 7. The negative logarithm of the likelihood as a function of M_A.

theoretical cross section must be corrected in order to compare with data. A Monte Carlo program was written to compute the muon detection efficiency (approximately 50%) as a function of Q^2. Previously we have computed the total number of $\bar{\nu}p \to \mu^+ n\pi^0$ as 11 ± 3 events (Sec. IV). In the reduced fiducial volume for quasielastic reactions we expect 8 ± 3 events. Because of the muon detection probability only 4 ± 2 of these will be included in the quasielastic sample. We assume these background events have the same Q^2 dependence as $\bar{\nu}p \to \mu^+ p\pi^-$, which we have experimentally measured (see Fig. 6).

As a check on this background estimate, we normalize the theoretical cross section $d\sigma/dQ^2$ for quasielastic events ($M_A \sim 1.0$) to the experimental data at $Q^2 = 0$, where the background from
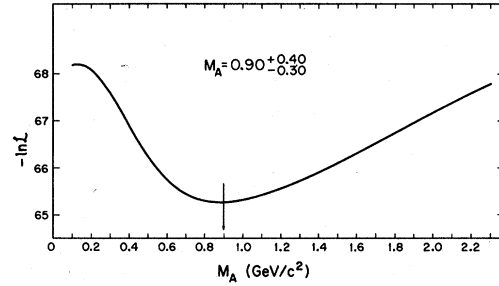
$\bar{\nu}p \to \mu^+ n\pi^0$ is small (15%). The difference between the data and this normalized quasielastic cross section is 4.5 ± 2.0 events, in good agreement with previous estimates of the background.

For 13 ± 6 events the cross section for quasielastic interactions becomes

$$(\bar{\nu}p \to \mu^+ n) = (0.5 \pm 0.2) \times 10^{-38} \text{ cm}^2$$

at the average $\bar{\nu}$ energy of 1.3 GeV. The theoretical value for this cross section ($M_A = 0.9$ GeV/c^2) is 0.44×10^{-38} cm^2, in agreement with the experimental result.

We use the maximum-likelihood method to extract the best value for the axial-vector mass M_A. The probability p_i of obtaining an event with a particular Q_i^2 from an antineutrino of energy E_i is

$$p_i = \frac{d\sigma/dQ^2(Q_i^2, E_i, M_A)W(Q_i^2) + d\sigma'/dQ^2(Q_i^2)W(Q_i^2)}{\int [d\sigma/dQ^2(Q^2, E_i, M_A)W(Q^2) + d\sigma'/dQ^2(Q^2)W(Q^2)]dQ^2} ,$$

where $d\sigma/dQ^2$ is the quasielastic cross section as given in (3), $d\sigma'/dQ^2$ is the experimental cross section for $\bar{\nu}p \to \mu^+ n\pi^0$ (assumed to have the same q^2 dependence as $\bar{\nu}p \to \mu^+ p\pi^-$), normalized to the expected $\bar{\nu}p \to \mu^+ n\pi^0$ contamination, and $W(Q_i^2)$ is the muon detection efficiency. The likelihood is defined

$$L = \prod_{i=1}^{17} p_i$$

and is flux independent. The negative logarithm of this likelihood function is shown as a function of M_A in Fig. 7. The result gives

$$M_A = (0.9^{+0.4}_{-0.3}) \text{ GeV}/c^2$$

in agreement with theoretical expectation, $M_A = 1.18$ GeV/c^2, from current algebra.[16] The only

antineutrino quasielastic measurement[4] gives $M_A = 0.91 \pm 0.04$ GeV/c^2 and the most recent neutrino measurements[11,12] of $\nu n \to \mu^- p$ give $M_A = 0.98 \pm 0.08$ and $M_A = 1.08 \pm 0.08$ GeV/c^2, in agreement with this experiment.

*Present address: University of Wisconsin, Madison, Wisc. 53706.

†Present address: University of Crete, Heraklion, Crete, Greece.

‡Present address: 1927 Commonwealth Avenue, Madison, Wisc.

[1] J. Blietschau *et al.*, Nucl. Phys. B118, 218 (1977).

[2] O. Erriquez *et al.*, Phys. Lett. 73B, 350 (1978).

[3] O. Erriquez *et al.*, Nucl. Phys. B140, 123 (1978).

[4] N. Armenise *et al.*, Nucl. Phys. B152, 365 (1979).

[5] O. Erriquez *et al.*, Phys. Lett. 80B, 209 (1979).

[6] Y. Rjabov, in *Proceedings of the 19th International Conference on High Energy Physics, Tokyo, 1978,* edited by S. Homma, M. Kawaguchi, and H. Miyazawa (Phys. Soc. of Japan, Tokyo, 1979), p. 319.

[7] For earlier references see P. Musset and J. P. Vialle, Phys. Rep. 39, 1 (1978).

[8] S. Barish *et al.*, Phys. Rev. D 16, 3103 (1977).

[9] E. Cazzoli *et al.*, Phys. Rev. Lett. 34, 1125 (1975).

[10] A. M. Cnops *et al.*, Phys. Rev. Lett. 42, 197 (1979).

[11] M. Derrick *et al.*, in *Proceedings of the Topical Conference on Neutrino Physics at Accelerators, Oxford, 1978,* edited by A. G. Michette and P. B. Renton (Rutherford Laboratory, Chilton, Didcot, Oxfordshire, England, 1978), p. 58.

[12] A. M. Cnops *et al.*, in *Proceedings of the Topical Conference on Neutrino Physics at Accelerators, Oxford, 1978* (Ref. 11), p. 62.

[13] M. J. Murtagh (private communication).

[14] N. Cabibbo and F. Chilton, Phys. Rev. 137B, 1628 (1965).

[15] S. Adler, Phys. Rev. D 12, 2644 (1975).

[16] S. Weinberg, Phys. Rev. Lett. 18, 507 (1967).